Dimensioning the Equipment of a Wave Farm: Energy Storage and Cables

Anne Blavette, Dara O'Sullivan, Tony Lewis, Michael Egan

Dimensioning the Equipment of a Wave Farm: Energy Storage and Cables

Anne Blavette, Dara L. O'Sullivan, Tony W. Lewis, Michael G. Egan

***Abstract*—Still largely untapped, wave energy may represent an important share in the energy mix of many countries in the future. However, the power fluctuations generated by most wave energy devices with little to no storage means, or without suitable control strategies, may cause power quality issues that must be solved before large wave energy farms are allowed to connect to the network. For instance, large power fluctuations may induce an excessive level of flicker in the distribution networks to which they are currently envisaged to be connected. Although storage appears to be a technically feasible solution, the minimum amount of storage required for a wave farm to become grid compliant with respect to typical flicker requirements is still unknown and is therefore investigated. This study constitutes the first part of the paper. Another issue, on which the second part of this paper focuses, concerns the optimal dimensioning of wave farm electrical components which is traditionally performed assuming steady-state conditions (i.e. constant current level), and it thus irrelevant in the case of wave farms outputting power fluctuations of significant amplitude. Hence, a second study, whose results are presented in this paper, focuses on the minimum current rating for which a submarine cable may be safely operated without thermal overloading. Addressing both these issues is essential to the economic viability of a wave farm as the cost of both storage means and electrical components is highly dependent on their rating and may represent a significant percentage of the capital expenditure.**

***Index Terms*—Storage, power quality, cable dimensioning**

I. Introduction

Flicker was identified as an important issue which may require the use of energy storage means or dedicated control strategies to reduce its level at the point of common coupling (PCC) below the limits enforced by power system operators [**?**]. Several studies have investigated the efficiency of different energy storage means in reducing the power standard deviation [**?**] and the flicker level [**?**], [**?**] generated by a small to medium size wave farm (up to 20 MW). However, in all cases, the farm was connected to a relatively weak grid, which is more prone to be negatively affected by the injection of fluctuating power, or to an extremely strong grid which was not affected, as expected. Hence, in all these cases, the short-circuit ratio (S_{cr}) was either relatively high or low. It must be noted that the minimum energy capacity required for maintaining the flicker level below the grid operator's limit was also investigated, regardless of the grid strength, but only in the frame of a small size farm whose rated power was equal to 1 MW [**?**]. Hence, this paper investigates the minimum characteristics required from a storage means for maintaining the flicker level generated by a medium size wave farm, whose rated power is approximately equal to 20 MW, below typically enforced limits. Flicker generation being highly dependent on the network grid strength, the study was performed for a wide range of typical strength levels, both in terms of short-circuit ratios and of impedance angle $\Psi_k = arctan(X/R)$. As these limits may vary significantly from one country or region to another, a survey was conducted in a previous work [**?**] to determine both the most permissive and the most stringent limits among the requirements enforced by several grid operators. These two limits were retained for the study presented in this paper.

Exploiting the entire amount of wave energy available at a given site, including during periods presenting the most extreme wave conditions, may be detrimental from an economical perspective. Besides requiring a more robust wave energy device design, harnessing energy during the most energetic sea-states demands also a higher rated, and thus more expensive, power transmission equipment, in particular regarding the submarine export cables. A study focusing on wind energy suggested power generation curtailment during highly energetic conditions as a relevant option to decrease the wind farm's capital expenditure by reducing the cables' rating. It demonstrated indeed that the optimal power rating, from an economical point of view, of the wind farm's export cable was significantly less than the rated power (89% in this specific case) [**?**]. In similar fashion, the additional contribution of highly energetic sea-states to the annual electricity production of a wave farm is relatively negligible [**?**]. Hence, power generation curtailment may also be envisaged as a way to optimize the design of a wave farm.

A complementary approach to the curtailment method consists of estimating the minimum current rating required from a cable based on its thermal response. It is important to note that the current rating corresponds to the maximum temperature at which each of the cable components can be safely operated. However, it is usually determined based on steady-state calculations (thus assuming a constant current) which are not representative of, nor relevant to wave energy applications, considering the rapid current fluctuations generated by a wave farm compared to the very slow thermal response of a submarine cable, ranging usually between 2 min to 30 min [**?**], [**?**]. Consequently, it is expected that a cable rated at a significantly lower current level than the maximum power may be safely operated without thermal overloading,

A. Blavette is with the University of Nantes, France, e-mail: anne.blavette@gmail.com.

D. L. O'Sullivan is with Analog Devices, Cork, Ireland

T. W. Lewis is with Beaufort Research-HMRC, Cork, Ireland

M. G. Egan, now retired, was with the Electrical Engineering Department, University College Cork, Ireland.

Manuscript received MM DD, YYYY.

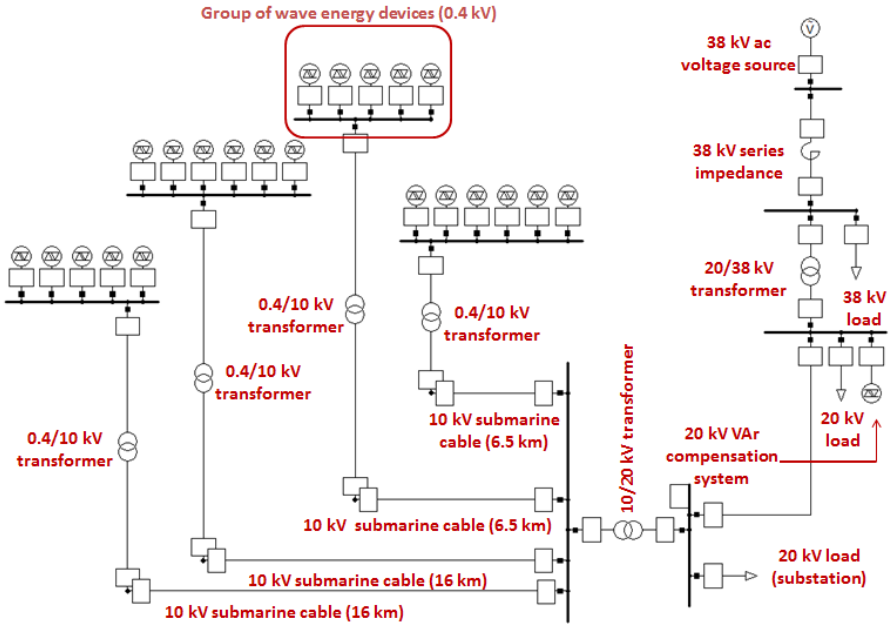

Fig. 1. Schematic overview of the electrical network model designed in PowerFactory

thus preventing a costly and useless over-rating. The second study of this paper investigates the minimum current to which a submarine cable can be rated (under conditions that will be described in more detail later in the paper) from a thermal loading perspective. Power system simulations were performed under DIgSILENT power system simulator "PowerFactory" and the thermal analysis of the cable was performed using models developed under Matlab-Simulink.

II. Modeling

A. Electrical network

The wave farm network model was inspired from the main characteristics of the national wave test site of Ireland located off Belmullet [**?**], which is also similar to most of the other test sites currently in operation or under development. This site will be connected to a particularly weak network having a short-circuit level estimated at 63 MVA and an impedance angle Ψ_k estimated at 69° in a previous work [**?**]. The farm is supplied by four submarine cables, two being 6.5 km long and the other two being 16 km long. Their capacitance and series impedance per meter (equal to 0.22 μF/m and 0.25+0.13i Ω/m respectively) are based on the cabling design studies performed at Beaufort Research-HMRC in conjunction with the site developer ESBI. An onshore substation, connected to the PCC through a 5 km overhead line, steps the voltage up from 10 kV to 20 kV. A 0.1 MVA load operated at 0.95 lagging power factor represents its consumption, and a generic storage means, described in more detail in Section **??**, is intended to smooth the farm's power output before it is injected into the grid. The PCC is located at the low voltage side of the 20/38 kV transformer, to which a VAr compensation system is also connected. This latter piece of equipment maintains power factor at a fixed value, equal to unity, according to typical grid operators' requirements. A 2.1 MVA load, also operated at 0.95 lagging power factor, located on the high voltage side of the 20/38 kV transformer, represents the consumption of a small size town of few thousands inhabitants.

Fig. **??** shows a schematic overview of the grid model designed in PowerFactory including the wave farm's internal network and the rest of the national/regional power system, modeled as a 38 kV voltage source in series with an impedance. The reactance and the resistance of this series impedance simulate different short-circuit levels and impedance angles, both of which are determining criteria regarding the strength of a network. A weak grid, whose power quality is more prone than a stronger grid to be negatively affected by the injection of power fluctuations, is usually characterized by a low value of either its short-circuit level or its impedance angle, or both. However, the strength of a given grid is relative to the characteristics of the injected power fluctuations. The ratio of the short-circuit level to the farm's maximum power, called the short-circuit ratio S_{cr}, is thus a more relevant criterion. The first study focusing on flicker was conducted for several values of the short-circuit ratio ranging from 3 (corresponding to a weak grid) to 15 (corresponding to a strong grid), and for four values of the impedance angle: 30°, 50°, 70° and 85°, as recommended in IEC standard 61400-21 [**?**].

B. Wave device power output

Experimental data in the form of electrical power output time series was provided as an outcome of the project CORES, standing for "Components for Ocean Renewable Energy Systems" [**?**]. This European FP7 project was based on a floating OWC (oscillating water column) device deployed offshore in the bay of Galway, Ireland during 3 months. The prototype was connected to a small on-board island grid independent from the national electrical network.

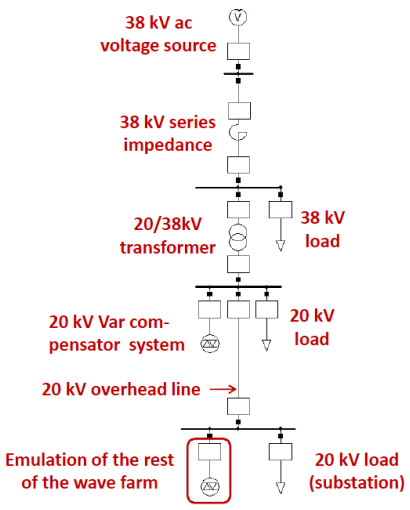

Fig. 2. Second electrical network model including storage

The full-scale significant wave height H_s and the zero-crossing period T_z of the time series retained for this study are equal to 4.6 m and 8.4 s respectively. This corresponds to moderate sea state conditions with respect to the national wave test site of Ireland which benefits from one of the highest wave energy potential in Europe [**?**]. However, it is also representative of a high energy sea state with respect to other sites presenting a milder sea climate. During the electricity generation period selected for this study, the generator was operated in constant speed control mode which means that, unlike in variable speed operation, inertial energy storage by means of speed control is not available. As a result, mechanical power peaks are converted directly into electrical power peaks, which is known to represent a worst case with respect to power quality impact [**?**].

C. Modeling of a multi-device wave farm

The wave farm is modeled based on 22 individual wave energy devices, leading to a full-scale rated power of 19.4 MW. A random time delay is applied to each generator's power profile in order to represent the effect of device aggregation on the power output of the farm.

D. Storage means

Initial power system simulations were performed based on the electrical model shown in Fig. **??**. In these simulations, no storage was available, i.e. no storage means was included in the model and the wave energy devices were operated in fixed speed mode. In order to evaluate the influence of storage on the flicker level induced by the wave energy farm, a second model, shown in Fig. **??** and including a generic storage means model, was used. In this model, the submarine cables, the 0.4/10 kV transformers and the wave energy devices are emulated by means of a built-in, controllable electrical machine model called "static generator".

The control frame of this machine, as developed in PowerFactory, is illustrated in Fig. **??**. The blocks "P-input" and

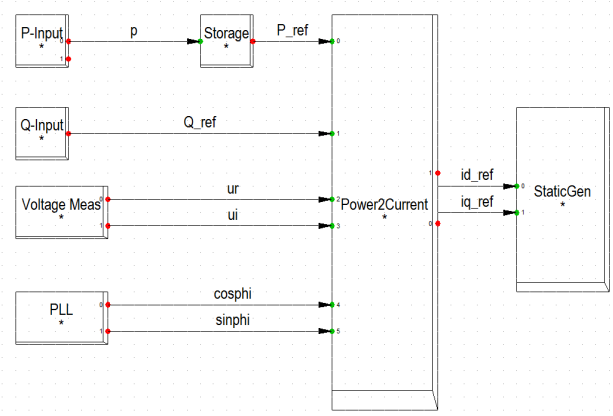

Fig. 3. Control frame of the generic storage means model

Storage means	Inertia time constant (s)	Description
Impulse turbine	1.7	Calculated from full-scale design concept [**?**]
Hydraulic accumulator	2	Volume: 50 L, pressure: 10-35 MPa [**?**]
Wells turbine	3.4	Calculated from full-scale design concept [**?**]
Supercapacitor bank	5.4-10.8	Combination of 13 modules using different control strategies (Maxwell Technologies BMOD0063 P125) [**?**]
Wells Turbine + flywheel	27	LIMPET assembly [**?**]
Reservoir	44	7000 m^3 reservoir [**?**]

TABLE I
INERTIA TIME CONSTANTS OF DIFFERENT STORAGE MEANS USED IN THE WAVE ENERGY INDUSTRY

"Q-input" output the active power and reactive power profiles flowing from the wave farm at the 10/20 kV substation as recorded from the initial simulations performed with the entire electrical network model shown in Fig. **??**. The "Storage" block is intended to represent a generic storage means modeled by a first-order filter of variable time constant τ [**?**] as:

$$P_{ref} = p\frac{1}{1+s\tau} \tag{1}$$

where P_{ref} is the output active power and p is the input active power. Depending on the value of time constant τ, the inertial response of different pieces of equipment can be represented, as shown in Table **??**.

The reactive power is not filtered so the profile output by block "Q-input" is equal to the reference reactive power Q_{ref}. Both reference powers P_{ref} and Q_{ref} are input to the "Power2Current" block which transforms the power references into direct and quadratic current references id_{ref} and iq_{ref} from which the static generator, represented by block "Static Gen", can be controlled. A voltage measurement block (outputting the real and imaginary voltage components u_r and u_i) as well as a PLL block (outputting the cosinus and sinus of angle Φ) are necessary to perform the transformation from power to current as:

$$i_r = \frac{P_{ref}}{u_r} - \frac{u_i}{(u_r^2+u_i^2)}\left(\frac{u_i}{u_r}P_{ref} - Q_{ref}\right) \tag{2}$$

$$i_i = \frac{u_r}{(u_r^2 + u_i^2)} \left(\frac{u_i}{u_r} P_{ref} - Q_{ref} \right) \quad (3)$$

where i_r and i_i are the real and imaginary current components respectively. The direct and quadratic current references id_{ref} and iq_{ref} can then be calculated as:

$$id_{ref} = i_r \cos\Phi + i_i \sin\Phi \quad (4)$$

$$iq_{ref} = -i_r \sin\Phi + i_i \cos\Phi \quad (5)$$

III. Flicker

A. Introduction

Flicker level is usually evaluated with respect to the perception of light intensity variations based on an incandescent light bulb model [**?**]. This may represent a worst case scenario regarding a number of lighting equipment types such as LEDs or fluorescent lamps, given their lower flicker response to low-frequency voltage modulation [**?**], [**?**]. However, in the absence of widely agreed guidelines or standards on the flicker response of different types of lighting and electrical equipment, the recommendations established by IEC standards 61000-4-15 and 61400-21 [**?**] were retained for developing the flickermeter used in the studies presented in this paper and whose design and performances were described in a previous work [**?**].

B. Flicker requirements

The most stringent as well as the most permissive limits in terms of short-term flicker level (Pst) as enforced in different countries were investigated in [**?**]. It appeared that the most stringent limit regarding P_{st} is enforced in the Republic of Ireland where the flicker contribution of wave farms at the PCC is expected not to exceed 0.35 when they are connected at distribution level. The most permissive limit in terms of P_{st}, enforced in several countries, regards the total flicker level and is equal to unity. These two limits were used as benchmarks for analyzing the simulation results.

IV. Methodology

A. Storage

Power system simulations were performed for several values of the storage means' time constant τ, namely 0 s (i.e. no storage), 1 s, 2 s and 3 s. Each voltage profile obtained was processed by means of the flickermeter to evaluate the corresponding short-term flicker level P_{st} at the PCC. Then, the minimum value required in terms of time constant τ for which P_{st} is maintained below the enforced limits was determined.

B. Cable rating

Considering the highly fluctuating electrical power output by wave farms, the maximum current flowing through a cable may not be a relevant indicator for selecting a suitable rating in the case of wave energy applications. Hence, it is important from an economical point of view to determine the minimum current rating at which a cable can be designed while avoiding thermal overloading.

Fig. 4. Nexans 2XS(FL)2YRAA RM (source: Nexans datasheet [**?**])

1) Ambient temperature: In the two studies composing the second part of this paper, the cable is assumed to be buried 1 meter below seabed at approximately 50 meter water depth which is the maximum water depth at which renewable offshore installations are (or are envisaged to be) deployed, due to both technical and economic constraints. The sea temperature at this depth, and thus the soil temperature 1 meter below seabed, may undergo significant annual variations similar in amplitude to these observed at the sea surface [**?**]. These temperature variations are also similar in amplitude and in phase to the average air temperature, as it was found at Malin Head, Ireland, for which available data on air and sea surface water monthly temperature (averaged over 1961 and 1990) [**?**], presented a high correlation factor (R^2=0.97).

Based on these observations, the simulations were performed for an ambient temperature θ_{amb} ranging between 0°C and 25°C in order to be representative of a wide spectrum of conditions under which submarine cables are expected to be operated. For the sake of comparison, the annual air temperature profile at different locations in northwestern Europe where wave farms are (or are envisaged to be) deployed were investigated. The investigations focused on the Wave Hub [**?**] and on the European Marine Energy Centre (EMEC) [**?**] located off Hayle and off Inverness respectively (both in the United Kingdom), and on the SEM-REV [**?**] off Le Croisic (France). The monthly average temperatures at these locations were found to range between 6°C and 19°C approximately [**?**], [**?**], [**?**].

2) Cable's design: The characteristics of the Nexans 2XS(FL)2YRAA RM cable [**?**], shown in Fig. **??**, match the requirements in terms of rated voltage (10 kV) and rated current (182 A) expected from the wave farm submarine cables, hence they were selected for developing the cable model used in the study. The cable includes three copper conductors insulated with cross-linked polyethylene (XLPE) and having each a copper screen. The sheath is made of polyethylene and the bedding of polypropylene yarn, as well as the serving. The surrounding armor is made of galvanized steel. Additional data necessary to perform the temperature rise calculations was estimated from information found in data sheets of other cables of similar structure, operating voltage and conductor size. The main parameters of the cable model are listed in Table **??**.

3) Thermal model: As mentioned earlier, the cable is assumed to be buried at the usual depth of 1 m below seabed. It is also assumed that the thermal resistance of the soil is constant, thus implying that it is homogenous in terms of

Parameter	Numerical value
Initial conductor diameter	8.2 mm
Operating voltage	12/20 (24) kV
Operating temperature	90°C
Nominal insulation thickness	5.5 mm
Screen section	16 mm^2
Nominal outer sheath thickness	2.5 mm
Armour thickness	3.15 mm
Maximum current when buried	199 A

TABLE II
CHARACTERISTICS OF THE CABLE SELECTED INITIALLY FOR THE ELECTRICAL NETWORK MODEL

Parameter	Definition	Numerical value
T_1	Thermal resistance between conductor and sheath	0.4929 K.m/W
T_2	Thermal resistance between sheath and armour	0.0890 K.m/W
T_3	Thermal resistance of external serving	0.1827 K.m/W
T_4	External thermal resistance	0.6783 K.m/W
W_d [1]	Dielectric loss	0.0041 W/m
λ_1 [2]	Loss ratio	$7.9151.10^{-7}$
λ_2 [2]	Loss ratio	$1.8093.10^{-7}$
R_cI^2 [2]	Thermal losses from one conductor	19 W/m

[1] Calculated based on a constant voltage equal to 10 kV
[2] Calculated based on a constant current equal to 100 A

TABLE III
THERMAL PARAMETERS OF THE SELECTED CABLE

materials and that no drying out occurs. Finally, the cable is assumed to be the sole source of heat in its close environement. The soil acts as a thermal reservoir: it absorbs all the heat released by the cable but its temperature is not affected.

Based on these observations, the method described in IEC standards 60287-1-1 [**?**] and 60287-2-1 [**?**] appeared to be relevant for the study presented in this paper. This method is initially intended for determining the maximum current rating of a cable under steady-state conditions, with respect to a permissible temperature range $\Delta\theta$, and based on the thermal properties of the cable's components, as well as on the external conditions.

The reverse approach was adopted in this study for determining the fictive temperature rise $\Delta\theta(t)$ resulting from the application of a fluctuating current $I(t)$. It is based on the following equation, given in IEC standard 60287-1-1, which describes the temperature rise $\Delta\theta$ of a conductor above ambient temperature due to a constant rms current I :

$$\Delta\theta = (I^2R_c + 0.5W_d)T_1 + [I^2R_c(1+\lambda_1) + W_d]nT_2 + [I^2R_c(1+\lambda_1+\lambda_2) + W_d]n(T_3+T_4) \quad (6)$$

where R_c is the conductor resistance per meter (Ω/m), W_d is the dielectric loss per meter (W/m), T_1, T_2, T_3 and T_4 are the thermal resistances of different parts of the conductor (K.m/W), n is the number of conductors in the cable, λ_1 and λ_2 are the loss ratios in different parts of the conductor to the total losses in all the conductors. The dielectric loss is calculated as:

$$W_d = \omega C U_0^2 \tan\delta \quad (7)$$

where C is the capacitance per meter and per phase, U_0 is the line-to-neutral voltage and $\tan\delta$ is the loss tangent. The dielectric loss is induced by the variations of the electrical field in a dielectric material. This phenomenon can be considered as instantaneous compared to the simulation time step used in the study (equal to 0.05 s). Hence, although (**??**) was defined initially for steady-state conditions, it is considered as applicable in the case of the dynamic simulations performed here. Consequently, the time-dependent dielectric loss is calculated from the rms voltage amplitude $V(t)$ computed with PowerFactory as:

$$W_d = \omega C_w V(t)^2 \tan\delta \quad (8)$$

The rest of the calculations was performed according to the recommendations of IEC standards 60287-1-1 and 62087-2-1. The results obtained for the thermal resistances T_1, T_2, T_3, T_4, for the dielectric loss W_d, for the loss ratios λ_1 and λ_2 and for the thermal losses from one conductor R_cI^2 are listed in Table **??**.

The cable thermal response was then modeled by filtering this temperature rise $\Delta\theta(t)$ by means of a first order low-pass filter whose time constant τ_t represents the cable's thermal response time, as found in the literature [**?**], [**?**]. Thermal time constants ranging usually between few minutes to few tens of minutes, analyses were performed for the following values: {5 min, 10 min, 15 min, 20 min, 25 min}. The initial current rating I_r of each of the four cables connecting the farm to the shore was selected based on the maximum power output by a cluster of wave devices in a submarine cable (equal to 3.1 MW) as:

$$I_r = \frac{P_r}{\sqrt{3}V} = \frac{3.1\times10^6}{\sqrt{3}\times10\times10^3} = 182\ A \quad (9)$$

The maximum permissible temperature was set to 90°C as it is the maximum operating temperature under steady-state conditions. This represents a worst case scenario, considering that the cable is designed to be operated at higher temperatures for limited periods of time. It may also be interesting to note that by limiting the maximum permissible temperature to its nominal operating temperature, no additional thermal aging effect compared to the steady-state case (due to excessive temperatures) needs to be considered.

The minimum current rating I_m for which the cable temperature remains below 90°C was evaluated by investigating the minimum conductor diameter d_{c_m} for which this condition is met. It is important to note that the conductor resistance per meter R_c increases in inverse proportion to the square of the conductor diameter d_c according to Pouillet's law as:

$$R_c = \frac{\rho}{S} \approx \frac{\rho}{\pi\left(\frac{d_c}{2}\right)^2} \quad (10)$$

where ρ is the conductor electrical resistivity and S is the conductor cross-sectional area. This generates higher Joules losses expressed as R_cI^2. Hence, the maximum temperature rise induced by a given current time series increases inversely to the conductor diameter. The minimum conductor diameter

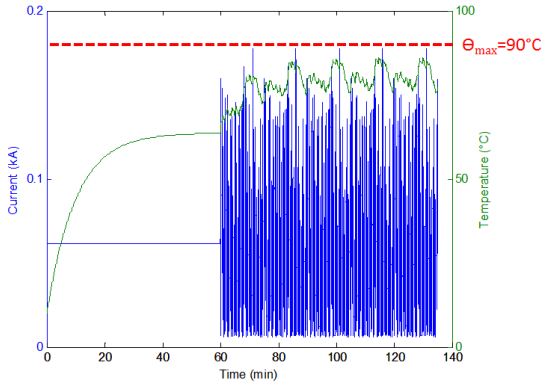

Fig. 5. Current loading and cable's temperature versus time (over-rated case)

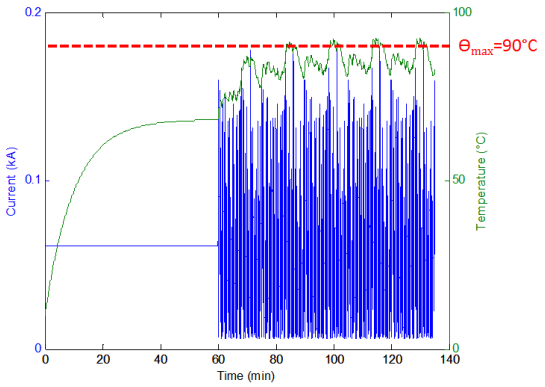

Fig. 6. Current loading and cable's temperature versus time (under-rated case)

d_{c_m} for which the cable's temperature does not exceed 90°C was determined iteratively. This approach is illustrated in Fig. **??** and Fig. **??**. These figures show the current loading in the cable as well as its conductor temperature versus time. In the case corresponding to Fig. **??**, the maximum temperature does not reach its limit. This means that the Joule losses are not excessive and that the resistance of the conductor, to which these losses are proportional, can be further increased, all the other parameters remaining constant. Consequently, the cable's conductor diameter d_c can be further reduced. Assuming reasonably that there exists a monotically increasing relation between the current rating and its conductor diameter, a cable having a lower conductor diameter is thus a cable designed for lower current rating, all the other parameters remaining the same. In other words, as the temperature was below its allowed limit, the cable could be considered as over-rated. However, in the case corresponding to Fig. **??**, the temperature exceeds its allowed limit. Hence, the cable can be considered as under-rated. The minimum conductor diameter d_{c_m} for which the cable's temperature does not exceed 90°C is comprised between the two diameter values.

It must be noted that each simulation is performed in two stages. First, a constant current loading is applied to the cable. The value of this current level was arbitrarely selected as equal to the average of the fluctuating current profile shown in Fig. **??** and Fig. **??** from time t=60 min. Then, the fluctuating current loading is applied. The role of the first phase of the simulation is simply to bring quickly the cable's temperature close to the range in which it is expected to find itself when the fluctuating current profile is applied, thus reducing the simulation time.

A graph linking the cross-sectional area of the cable conductor to its current rating was developed, as shown in Fig. **??**, based on technical data extracted from manufacturer datasheets [**?**], [**?**]. A best-fitting function was searched in order to approximate the current rating as a function of the conductor cross-sectional area. In order to improve its relevance, an ordinate in zero was added and approximated to zero, considering that the current level flowing through a conductor whose diameter converges to zero would also converge to zero. A 5$^{\text{th}}$ order polynomial was found to show a high correlation factor R^2 approximately equal to unity.

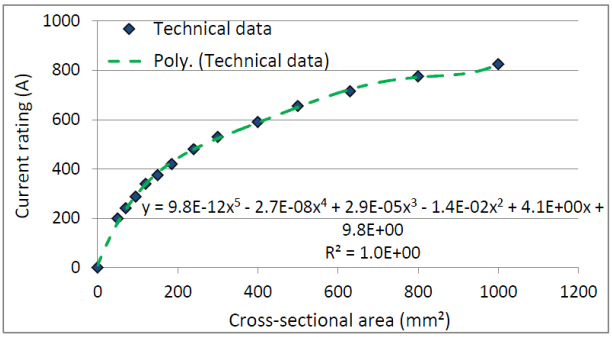

Fig. 7. Typical cable rating as a function of the conductor cross-sectional area S (technical data and 5$^{\text{th}}$ order polynomial approximation)

The values of the minimum current rating corresponding to the minimum conductor diameter d_{c_m} were found using this polynomial approximation.

V. Results

A. Storage

Using a storage means reduces considerably the voltage fluctuations at the PCC even for values of the time constant τ as low as 1 s. Consequently, flicker level P_{st} is also dramatically reduced, as illustrated in Fig. **??** which shows the flicker level for the considered range of short-circuit ratio S_{cr} and impedance angle Ψ_k. Although the flicker level may exceed the most permissive limit for values of the impedance angle Ψ_k up to 50° for the connection points with the lowest short-circuit ratio, a storage constant τ as low as 1 s is sufficient for reducing it below unity in this case. If the most stringent limit is enforced, then a storage constant τ equal to 3 s is required for the weakest grids. A storage constant τ equal to 1 s only is sufficient for reducing flicker below the most stringent limit for connection points whose impedance angle is equal to 70° for the weakest grids. In particular, a storage means' time constant of 1 s would be sufficient for a wave farm connected to the AMETS test site to be compliant with the Irish flicker requirement. This outcome is important as this situation constitutes a worst case scenario given the severity of the flicker requirements in Ireland as well as the weakness of the local grid at Belmullet. Connection points

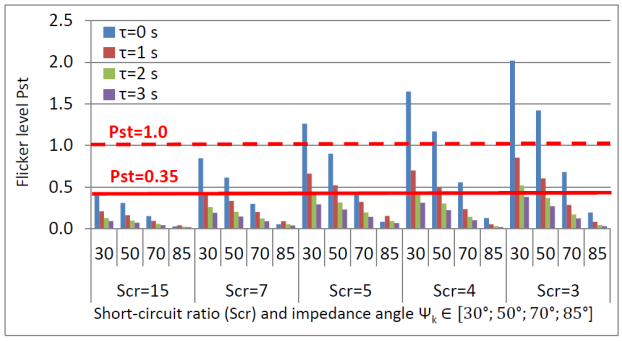

Fig. 8. Flicker level for several values of the storage means' time constant τ

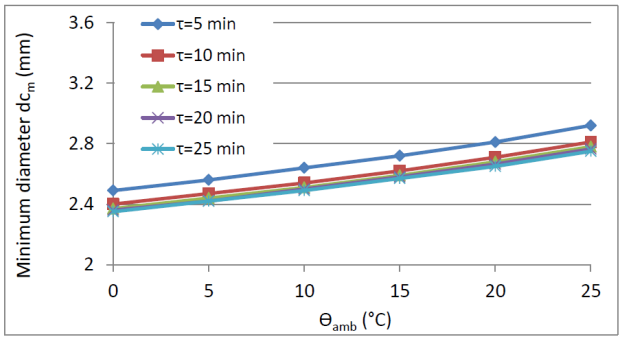

Fig. 9. Minimum conductor diameter d_{c_m} as a function of the ambient temperature θ_{amb} for different values of thermal constant τ_t

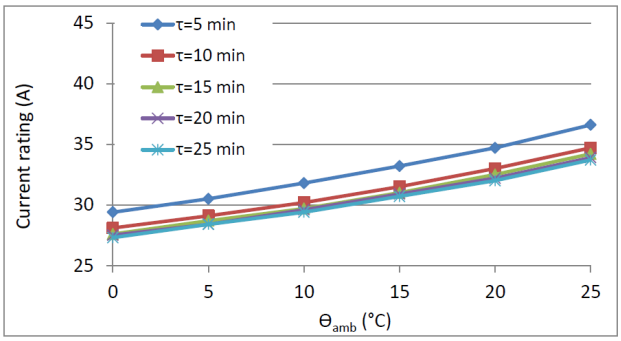

Fig. 10. Minimum current rating I_m as a function of the ambient temperature θ_{amb} for different values of thermal constant τ_t

whose impedance angle is equal to 85° and/or whose short-circuit ratio is greater than 15 do not require using a storage means to smooth the farm's power output as the flicker level obtained for this type of points is maintained below the most stringent limit in any case. Hence, in summary, a storage means of particularly low time constant τ may be sufficient for avoiding any flicker issue posed by the connection of a medium-size wave farm to a particularly weak grid. Inertia time constants of typical storage means used in the wave energy industry are listed in Table **??**. Knowing that a storage means of inertia time constant less than or equal to 3 s is sufficient to mitigate flicker, it can take the form of a hydraulic accumulator, of a small flywheel, of a supercapacitor bank or of variable speed control of air turbines in the case of OWCs. In other words, no large, dedicated storage structures such as a reservoir are necessary as far as flicker attenuation is concerned.

B. Cable rating

The simulation results confirmed that the cable selected initially was clearly over-rated with respect to the current time series considered in this study. Fig. **??** shows the minimum conductor diameter d_{c_m} as a function of the ambient temperature θ_{amb}. The minimum diameter d_{c_m} ranges between 2.35 mm and 2.92 mm which is indeed much smaller than the initial conductor diameter equal to 8.2 mm as shown in Table **??**. As expected, the required minimum diameter d_{c_m} increases as a function of the ambient temperature as the temperature of the cable is equal to summation of its temperature increase $\Delta\theta$ with the ambient temperature θ_{amb}. Hence, the higher the ambient temperature, the smaller is the margin allowed for the temperature rise $\Delta\theta$. Consequently, all other parameters remaining constant, the conductor resistance R_c must decrease (and hence diameter d_{c_m} increase) for the cable temperature not to exceed 90°C. The thermal time constant τ_t has also a significant influence on the minimum diameter d_{c_m} which can be explained as follows: the greater the thermal constant τ_t, the smoother the temperature profile, and hence the smaller the temperature peaks in terms of amplitude. This results in a lower maximum temperature and allows a smaller diameter cable to be used.

As detailed previously, the values of the minimum current rating I_m were calculated based on the 5$^{\text{th}}$ order polynomial approximation described in Section **??**. The results of the minimum current rating I_m as a function of the ambient temperature θ_{amb} are shown in Fig. **??**. It can be observed that the minimum current rating ranges between 27.3 A and 36.6 A, depending on the ambient temperature θ_{amb} and on the thermal constant τ_t. These values are expressed as a percentage of the average and of the maximum current flowing through the cable, equal to 62 A and 178 A respectively, in Table **??**. It is important to note that the minimum current rating I_m is equal to approximately half of the average current (ranging between 44% and 59%), which represents only 15% to 21% of the maximum current. This demonstrates that dimensioning a submarine cable based on the maximum current flowing through it leads to a useless over-sizing whereas the average current seems to be a more relevant criterion.

However, the results described in this section must be considered pragmatically. In practice, the conductor diameter of available submarine cables operated at this voltage level is usually greater than or equal to 8.2 mm (no cable of smaller diameter was found), which is much greater than the recommended diameter values. However, although the results obtained for an approximately 20 MW wave farm can be con-

	Average (62 A)	Maximum (178 A)
max(I_m)	59%	21%
min(I_m)	44%	15%

TABLE IV
MAXIMUM AND MINIMUM VALUE OF CURRENT RATING I_m (% OF THE AVERAGE AND MAXIMUM VALUES OF THE CURRENT TIME SERIES)

sidered as "fictive" as long as cables with a smaller conductor diameter are unavailable, the methodology developed as part of this work may be applied to cables included in wave farms of greater rated power. As mentioned previously, estimating the minimum cable rating more accurately in the case of wave energy applications may lead to a significant decrease in terms of capital expenditure.

VI. Conclusions

This paper presented two studies focusing on the dimensioning of a storage means and of electrical components, namely submarine cables, to be included in a wave energy farm. The first study was intended to determine the characteristics required from a storage means for maintaining the short-term flicker level at the PCC below limits enforced in a number of countries. The storage means was modeled generically by a first order low-pass filter of time constant τ. The minimum value required for this time constant τ, when necessary, was demonstrated to range between 1 s and 3 s, indicating that storage means such as a hydraulic accumulator, a small flywheel, a supercapacitor bank or the variable speed control of air turbines in the case of OWCs may be sufficient (independently or in combination) to maintain the flicker level induced by the wave farm under the maximum limit allowed by grid operators. In other words, no large, dedicated storage structures such as a reservoir are necessary as far as flicker attenuation is concerned. In particular, the connection of a wave farm to the AMETS test site proved to necessitate the use of a storage means whose time constant τ is equal to 1 s only. This is an important outcome of this study as the connection of a wave energy farm to the Irish test site constitutes a worst case scenario given the severity of the flicker requirements in Ireland and the weakness of the local grid of Belmullet.

This study investigated also the dimensioning of submarine cables from a thermal perspective. A method based on IEC standards was developed as part of this work and was presented in this paper. It was demonstrated that basing the dimensioning of a submarine cable on the maximum current flowing through it leads to an unnecessary over-sizing and is thus irrelevant in the case of wave energy applications. In addition, the average current appears to be a more relevant criterion. More specifically, the results presented in this paper showed that the current rating obtained through this method is equal to approximately half of the average current, ranging between 44% and 59%. This is the second important outcome of this paper, as estimating more accurately the minimum current rating of submarine cables may lead to a significant decrease in terms of capital expenditure. Further work will be performed on the experimental validation of this method in the near future.

Acknowledgment

The authors wish to acknowledge members of the FP7 project CORES team (RCN 41815) for their technical help. Financial support from Science Foundation Ireland through the Charles Parsons Initiative is also gratefully acknowledged.

References

[1] A. Blavette *et al.*, "Impact of a medium-size wave farm on grids of different strength levels", *IEEE Trans. on Power Systems*, p. 917-923, March 2014.

[2] A. Nambiar *et al.*, "Effects of array configuration, network impacts and mitigation of arrays of wave energy converters connected to weak, rural electricity networks", *Proc. 3rd Int. Conf. Ocean Energy, Spain*, 2010.

[3] D. O'Sullivan *et al.*, "Case studies on the benefits of energy storage for power quality enhancement: oscillating water column arrays", *Proc. 4th Int. Conf. on Ocean Energy, Dublin, Ireland*, 2012.

[4] M. Santos *et al.*, "Case Study on the benefits of energy storage for power quality enhancement: point absorber arrays", *Proc. 4th Int. Conf. on Ocean Energy, Dublin, Ireland*, 2012.

[5] J. Aubry, "Optimisation du dimensionnement d'une chaîne de conversion électrique directe incluant un système de lissage de production par supercondensateurs. Application au houlogénérateur SEAREV", *PhD thesis, Ecole Nationale Supérieure de Cachan, France*, 2011.

[6] Econnect and National Grid, "Round 3 Offshore Wind Farm Connection Study", *a report prepared by econnect and National grid for the Crown Estate*, 2009.

[7] F. Sharkey *et al.*, "Dynamic electrical ratings and the economics of capacity factor for wave energy converter arrays", in *Proc. of the 9th European Wave and Tidal Energy Conf., Southampton, UK*, 2011.

[8] R. Adapa and D. Douglass. "Dynamic thermal ratings: monitors and calculation methods". *Proc. of the IEEE Power Eng. Society Inaugural Conf. and Exposition in Africa*, p.163-167, 2005.

[9] J. Hosek. "Dynamic thermal rating of power transmission lines and renewable resources.", ES1002 : Workshop March 22nd-23rd, 2011.

[10] Website of the SEAI, http://www.seai.ie/.

[11] A. Blavette, "Grid integration of wave energy & generic modelling of ocean devices for power system studies", *PhD thesis, University College Cork, Ireland*, 2013.

[12] IEC standard 61400-21, "Measurement and assessment of power quality characteristics of grid connected wind turbines", 08/2008.

[13] R. Alcorn, *et al.*, "FP7 EU funded CORES wave energy project: a coordinators perspective on the Galway Bay sea trials", *Underwater Technology, Vol. 32, No. 1, pp. 5159*, 2014.

[14] B. G. Cahill *et al.*, "Wave energy resource characterization of the Atlantic Marine Energy Test Site", *Proc. of the 9th European Wave and Tidal Energy Conf., Southampton, UK*, 2011.

[15] T. Ackermann, "Wind power in power systems", *Wiley & Sons*, 2nd edition., 2012.

[16] A. Blavette *et al.*, "A novel method for estimating the flicker level generated by a wave energy farm composed of devices operated in variable speed mode", *Proc. of the Int. EVER'14 Conf., Monaco, 2014.*

[17] D. O'Sullivan *et al.*, "Dynamic characteristics of wave and tidal energy converters & a recommended structure for development of a generic model for grid connection", *OES-IA Annex III*, 2010.

[18] IEC standard 61000-4-15, "Electromagnetic compatibility (EMC) - Part 4-15: Testing and measurement techniques - Flickermeter", 08/2010.

[19] C. Rong *et al.*, "Flickermeter used for different types of lamps", *Proc. of the 9th Int. Conf. on Electrical Power Quality and Utilisation*, 2007.

[20] W. Heffernan *et al.*, "LED Replacement for Fluorescent Tube Lighting", *Proc. of the 2007 Australasian Universities Power Eng. Conf.*, 2007.

[21] Marine Scotland, "Scotland's Marine Atlas: Information for The National Marine Plan", 2011.

[22] MetEireann, http://www.met.ie/climate-ireland/30year-averages.asp, accessed June, 19 2014.

[23] Website of WaveHub: www.wavehub.co.uk/.

[24] Website of EMEC: www.emec.org.uk.

[25] Website of SEM-REV: www.semrev.fr

[26] Météo-Bretagne, town: St-Nazaire, accessed June, 25 2014.

[27] MetOffice, http://www.metoffice.gov.uk/public/weather/climate/, accessed June, 19 2014.

[28] Nexans data sheet, technical reference: 2XS(FL)2YRAA RM 12/20 (24)kV, "3 core XLPE-insulated cables with PE sheath and armouring"

[29] IEC standard 60287-1-1, "Electric cables : Calculation of the current rating. Part 1-1: Current rating equations (100 % load factor) and calculation of losses", ed.2.0, 12/2006.

[30] IEC standard 60287-2-1, "Electric cables - Calculation of the current rating - Part 2: Thermal resistance", ed1.2 Consol. with am1&2, 05/2006.

[31] Nexans, "Submarine cable 10kV, 6/10 (12)kV 3 core Copper XLPE cable, Cu-screen, Al/PE-sheath, Armouring"

[32] Universal Cable, "XLPE insulated power cables"

[33] ABB, "XLPE Submarine Cable Systems Attachment to XLPE Land Cable Systems - User's Guide", rev. 5